

Current-driven and field-driven domain walls at nonzero temperature

M.E. Lucassen,* H.J. van Driel, C. Morais Smith, and R.A. Duine
*Institute for Theoretical Physics, Utrecht University,
Leuvenlaan 4, 3584 CE Utrecht, The Netherlands*
(Dated: October 26, 2018)

We present a model for the dynamics of current- and field-driven domain-wall lines at nonzero temperature. We compute thermally-averaged drift velocities from the Fokker-Planck equation that describes the nonzero-temperature dynamics of the domain wall. As special limits of this general description, we describe rigid domain walls as well as vortex domain walls. In these limits, we determine also depinning times of the domain wall from an extrinsic pinning potential. We compare our theory with previous theoretical and experimental work.

PACS numbers: 72.25.Pn, 72.15.Gd, 72.70.+m

I. INTRODUCTION

Current-driven domain wall motion was first predicted and observed by Berger in the eighties.^{1,2} It was not until the discovery, in the nineties, of the spin transfer torque mechanism,^{3,4} that research on current-driven domain walls took off. Spin transfer torques on a domain wall can be understood on an intuitive level: the electrons which constitute the current have spin, and this spin rotates when it passes through the domain wall, as it aligns with the domain wall magnetization. By conservation of spin, there is an opposite torque on the magnetization of the domain wall, which leads to a net displacement of the domain wall in the same direction as the electric current. Later, to explain some discrepancies with experiments, a so-called dissipative spin transfer torque (sometimes referred to as the non-adiabatic spin transfer torque) was added to the model.^{5,6} The value of the dimensionless parameter β , which gives the strength of this torque, has been the subject of much debate. By now it is generally accepted that β is of the same order as α , the Gilbert damping parameter, but not necessarily equal to it.^{7,8,9,10,11} Furthermore, neither β nor α needs to be constant. They depend on the properties of the material and are most likely also temperature dependent.

Several properties of current-driven domain walls have been studied. One particular subject of interest is the velocity of the domain wall. The effect of an external pinning potential and the depinning behavior, both without and with thermal fluctuations, were investigated experimentally.^{12,13,14} There is also interest in more complex, higher dimensional domain wall models, like vortex walls.^{15,16,17} These are especially attractive from an experimental point of view since their dynamics, such as precession in a potential and transformations between vortex walls and transverse walls, can be directly observed.^{7,18,19,20}

With a few exceptions,^{21,22,23,24,25} most theoretical papers are restricted to the zero-temperature case. This is unfortunate, since experiments on current-driven domain walls are usually done at room temperature, and the relatively large current will heat up the sample even further. Furthermore, especially in the presence of a pinning po-

tential, thermal fluctuations are anything but negligible. Domain pinning can be necessary, for instance to precisely locate a domain wall, but thermal depinning can also be useful to lower the critical current. This means that it is very important to understand the influence of thermal fluctuations on the behavior of the domain wall precisely and thoroughly. Here, we present a unified picture of previous work on domain wall motion at nonzero temperature that involved two of us, as well as new results following from this unified picture.

We start this paper with the Landau-Lifschitz-Gilbert equation, including both the reactive and the dissipative spin transfer torques. In Section II, we apply a variational principle to derive the general equations of motion for a domain-wall line including thermal fluctuations. In Section III we investigate the velocity of current-driven and field-driven rigid domain walls at nonzero temperature, while in Section IV we look at vortex domain walls in more detail. Both the rigid and the vortex domain wall are special cases of the general description given in Section II. In both sections, we start with the zero-temperature case, and then investigate the influence of thermal fluctuations. Pinning potentials are included in both models, and we examine thermal depinning. Each section is divided into three subsections: one in which the model is described, one in which we present our results, and a final one to make a comparison with other work.

II. DOMAIN-WALL LINES

In this section, we derive the equations of motion for a domain-wall line in a more detailed way than in previous work²¹ and present new results obtained from this model. We derive the Fokker-Planck equation of the system, and determine the stochastic behavior under the influence of temperature. The model is then considered in the absence of extrinsic pinning so that there is only intrinsic pinning due to magnetic anisotropy. We determine the drift velocity of the domain wall as a function of the current through the system. Finally, we compare our model with other theoretical and experimental work available in the literature.

A. Model

Magnetization dynamics including spin-transfer torques are described by the Landau-Lifschitz-Gilbert equation^{3,4}

$$\left(\frac{\partial}{\partial t} + \vec{v}_s \cdot \vec{\nabla}\right) \mathbf{\Omega} = \mathbf{\Omega} \times \mathbf{H} - \alpha \mathbf{\Omega} \times \left(\frac{\partial}{\partial t} + \frac{\beta}{\alpha} \vec{v}_s \cdot \vec{\nabla}\right) \mathbf{\Omega}, \quad (1)$$

where $\mathbf{\Omega}$ is a unit vector in the direction of the magnetization. In this expression, the first term on the r.h.s. contains a contribution due to the effective field, which is written as the functional derivative of the micromagnetic energy functional of the system and an external magnetic field $\mathbf{H}(\vec{x}, t) = -\delta E_{\text{MM}}[\mathbf{\Omega}(\vec{x}, t)]/\hbar \delta \mathbf{\Omega}(\vec{x}, t) + g \mathbf{B}_{\text{ext}}(\vec{x}, t)/\hbar$. For clarity, we denote positions in three-dimensional space with an arrow, and the directions of the magnetization by bold symbols. The second term describes Gilbert damping, which is characterized by the dimensionless parameter α . The term proportional to \vec{v}_s on the l.h.s. is the reactive spin-transfer torque. The term proportional to $\beta \vec{v}_s$ on the r.h.s. corresponds to the dissipative spin-transfer torque and is characterized by the dimensionless parameter β . The velocity \vec{v}_s is given by $\vec{v}_s = -a^3 P \vec{J}_c / |e|$, where a is the lattice constant, \vec{J}_c is the charge current and P is its spin polarization. To facilitate a variational approach, we note that the Landau-Lifschitz-Gilbert equation is obtained from

$$\frac{\delta S}{\delta \mathbf{\Omega}(\vec{x}, t)} = \frac{\delta R}{\delta \mathbf{\Omega}(\vec{x}, t)}, \quad (2)$$

where R is a dissipation functional, and where $S = S_0 + S_{\text{drive}}$ denotes the action of the system. The dot is a time derivative $\dot{\mathbf{\Omega}} \equiv \partial \mathbf{\Omega} / \partial t$. The action for the magnetization dynamics in the absence of current and field is given by

$$\begin{aligned} S_0[\mathbf{\Omega}(\vec{x}, t)] &= \int dt \int \frac{d^3 x}{a^3} \left\{ \hbar \mathbf{A}(\mathbf{\Omega}(\vec{x}, t)) \cdot \frac{\partial \mathbf{\Omega}(\vec{x}, t)}{\partial t} \right. \\ &\quad \left. + J \mathbf{\Omega}(\vec{x}, t) \cdot \vec{\nabla}^2 \mathbf{\Omega}(\vec{x}, t) - K_{\perp} \Omega_y^2(\vec{x}, t) + K_z \Omega_z^2(\vec{x}, t) \right\} \\ &\equiv \int dt \left\{ \int \frac{d^3 x}{a^3} \hbar \mathbf{A}(\mathbf{\Omega}(\vec{x}, t)) \cdot \frac{\partial \mathbf{\Omega}(\vec{x}, t)}{\partial t} - E_{\text{MM}}[\mathbf{\Omega}(\vec{x}, t)] \right\}. \end{aligned} \quad (3)$$

In this expression, J is the spin stiffness, $K_{\perp} > 0$ and $K_z > 0$ are the hard- and easy-axis anisotropy, respectively. The function $\mathbf{A}(\mathbf{\Omega})$ is the vector potential of a magnetic monopole which obeys $\nabla_{\mathbf{\Omega}} \times \mathbf{A}(\mathbf{\Omega}) = \mathbf{\Omega}$ and is required to reproduce the precessional motion of $\mathbf{\Omega}(\vec{x}, t)$ around the effective field.

The external field $\mathbf{B}_{\text{ext}}(\vec{x}, t)$ and the reactive spin-transfer torque are determined from the action $S_{\text{drive}}[\mathbf{\Omega}(\vec{x}, t)]$. We take the external magnetic field to be spatially homogeneous and time independent

$\mathbf{B}_{\text{ext}}(\vec{x}, t) = \mathbf{B}_{\text{ext}}$. The action is given by

$$S_{\text{drive}}[\mathbf{\Omega}(\vec{x}, t)] = \int dt \int \frac{d^3 x}{a^3} \left\{ g \mathbf{B}_{\text{ext}} \cdot \mathbf{\Omega}(\vec{x}, t) + \mathbf{A}(\mathbf{\Omega}) \cdot \left(\vec{v}_s \cdot \vec{\nabla}\right) \mathbf{\Omega}(\vec{x}, t) \right\}, \quad (4)$$

with g a positive constant. The dissipation functional that describes the dissipative spin-transfer torque and the Gilbert damping is written as

$$R[\mathbf{\Omega}(\vec{x}, t)] = \frac{\alpha \hbar}{2} \int dt \int \frac{d^3 x}{a^3} \left[\left(\frac{\partial}{\partial t} + \frac{\beta}{\alpha} \vec{v}_s \cdot \vec{\nabla}\right) \mathbf{\Omega}(\vec{x}, t) \right]^2. \quad (5)$$

As the last ingredient, we take into account thermal fluctuations. We add to the effective field in Eq. (1) stochastic contributions \mathbf{h} such that $\mathbf{H} \rightarrow \mathbf{H} + \mathbf{h}$, where \mathbf{h} has white-noise correlations

$$\langle h_i(\vec{x}, t) h_j(\vec{x}', t') \rangle = \sigma_{ij} \delta(\vec{x} - \vec{x}') \delta(t - t'), \quad (6)$$

$$\langle h_i(\vec{x}, t) \rangle = 0, \quad (7)$$

and where the indices $i, j \in \{x, y, z\}$ label Cartesian coordinates. The strength σ_{ij} is given by the fluctuation-dissipation theorem $\sigma_{ij} = \delta_{ij} 2\alpha k_B T a^3 / \hbar$, which assures that, in the absence of field and current, the Boltzmann equilibrium distribution

$$P_{\text{eq}}[\mathbf{\Omega}] \propto e^{-E_{\text{MM}}[\mathbf{\Omega}] / k_B T}, \quad (8)$$

is reached after sufficiently long times. In principle, Eqs. (2–6) describe the full magnetization dynamics. Obtaining results on finite-temperature average drift velocities of domain walls is however very cumbersome, especially in the presence of extrinsic pinning. We therefore use a variational method.

We obtain the specific form of our variational ansatz by varying the action in Eq. (3) for a time-independent magnetization. Using $\mathbf{\Omega} = (\sin \theta \cos \phi, \sin \theta \sin \phi, \cos \theta)$ we find $\theta'' = (K_z / J) \sin^2 \theta$,²⁶ where the primes denote derivatives with respect to x . This equation has domain-wall solutions $\tan(\theta/2) = \exp\{\pm[x - X]/\lambda\}$ and $\phi \in \{0, \pi\}$, where $\lambda = \sqrt{J/K_z}$ is the domain-wall width and X is the position of the domain wall.

The variational *ansatz* we use is $\tan(\theta_{\text{dw}}/2) = \exp\{[x - X(z, t)]/\lambda\}$ and $\phi = \phi_0(z, t)$. A domain wall is now described by two collective coordinates $X(z, t)$ and $\phi_0(z, t)$ that represent the position of the domain wall line and the chirality at this position, respectively. Note that z is the coordinate along the line, and also that there are other possibilities for the exact form of the *ansatz*, such as choosing a different domain-wall charge.

We choose the magnetic field pointing in the positive z direction $\mathbf{B}_{\text{ext}} = B_z \hat{z}$, $B_z > 0$. Furthermore, the current is taken in the positive x direction. We find that the

action in terms of the collective coordinates $X(z, t)$ and $\phi_0(z, t)$ is then given by

$$S[X, \phi_0] = -N\hbar \int dt \int \frac{dz}{L_z} \left(\frac{X}{\lambda} \dot{\phi}_0 + \frac{K_{\perp}}{\hbar} \sin^2 \phi_0 + \frac{J}{\hbar} \frac{(X')^2}{\lambda^2} + \frac{J}{\hbar} (\phi_0')^2 - \frac{gB_z}{\hbar} \frac{X}{\lambda} + \frac{v_s}{\lambda} \phi_0 \right), \quad (9)$$

where $N = 2\lambda L_y L_z / a^3$ is the number of magnetic moments in a domain wall, with L_y, L_z the length of the sample in the y and z direction, respectively. We now substitute the *ansatz* in Eq. (5) to obtain the dissipation functional as a function of the collective coordinates

$$R[X, \phi_0] = N \frac{\alpha \hbar}{2} \int dt \int \frac{dz}{L_z} \left[\left(\frac{\dot{X}}{\lambda} - \frac{\beta v_s}{\alpha \lambda} \right)^2 + \dot{\phi}_0^2 \right]. \quad (10)$$

Upon variation of the total action in Eq. (9) with respect to X and ϕ_0 , and setting this equal to the variation of the dissipation function in Eq. (10) with respect to \dot{X} and $\dot{\phi}_0$, respectively, we obtain equations of motion for the collective coordinates

$$\dot{\phi}_0 + \alpha \frac{\dot{X}}{\lambda} = \frac{2J}{\hbar} \frac{X''}{\lambda} + \beta \frac{v_s}{\lambda} + \frac{gB_z}{\hbar}, \quad (11)$$

$$\frac{\dot{X}}{\lambda} - \alpha \dot{\phi}_0 = -\frac{2J}{\hbar} \phi_0'' + \frac{K_{\perp}}{\hbar} \sin(2\phi_0) + \frac{v_s}{\lambda}. \quad (12)$$

We now add thermal fluctuations that contribute as stochastic terms to Eqs. (11) and (12), so that we obtain Langevin equations

$$\dot{\phi}_0(z, t) + \alpha \frac{\dot{X}(z, t)}{\lambda} = -\frac{L_z \lambda}{\hbar N} \frac{\delta V_{\text{eff}}[X, \phi_0]}{\delta X(z)} + \eta_X(z, t), \quad (13)$$

$$\frac{\dot{X}(z, t)}{\lambda} - \alpha \dot{\phi}_0(z, t) = \frac{L_z}{\hbar N} \frac{\delta V_{\text{eff}}[X, \phi_0]}{\delta \phi_0(z)} + \eta_{\phi_0}(z, t). \quad (14)$$

Here we take functional derivatives of an effective potential that is a functional of $X(z)$ and $\phi_0(z)$. Allowing for an arbitrary potential $V_{\text{dis}}(X, \phi_0)$ due to disorder and inhomogeneities, this effective potential is given by

$$V_{\text{eff}}[X, \phi_0] = -\hbar N \int_0^{L_z} \frac{dz}{L_z} \left[-\frac{J}{\hbar} \left(\frac{X'^2}{\lambda^2} + \phi_0'^2 \right) + \frac{K_{\perp}}{2\hbar} \cos(2\phi_0) + \frac{v_s}{\lambda} \left(\beta \frac{X}{\lambda} - \phi_0 \right) + \frac{gB_z}{\hbar} \frac{X}{\lambda} \right] + V_{\text{dis}}(X, \phi_0), \quad (15)$$

and also includes contributions from the micromagnetic energy functional, the external field, and spin-transfer

torques. Note that in the absence of current, field and disorder, the potential in Eq. (15) is exactly the total micromagnetic energy $E_{\text{MM}}[\mathbf{\Omega}_{\text{dw}}] = V_{\text{eff}}[X, \phi_0]$.

The noise in Eqs. (13) and (14) obeys $\langle \eta_i(z, t) \eta_j(z', t') \rangle = \sigma \delta_{ij} \delta(t - t') \delta(z - z')$ and $\langle \eta_i(z, t) \rangle = 0$, where $\{i, j\} \in \{X, \phi_0\}$. The strength σ can be determined from the Fokker-Planck equation, which for the Langevin equations (13) and (14) is given by²⁷

$$(1 + \alpha^2) \frac{\partial P[X, \phi_0]}{\partial t} = \frac{1}{\hbar} \int_0^{L_z} \frac{dz}{L_z} \left\{ \frac{\delta}{\delta \phi_0} \left[\left(\frac{\alpha}{N} \frac{\delta V_{\text{eff}}}{\delta \phi_0} + \frac{\lambda}{N} \frac{\delta V_{\text{eff}}}{\delta X} \right) P[X, \phi_0] \right] + \lambda \frac{\delta}{\delta X} \left[\left(\frac{\alpha \lambda}{N} \frac{\delta V_{\text{eff}}}{\delta X} - \frac{1}{N} \frac{\delta V_{\text{eff}}}{\delta \phi_0} \right) P[X, \phi_0] \right] + \frac{\sigma}{2} \left(\lambda^2 \frac{\delta^2}{\delta X^2} + \frac{\delta^2}{\delta \phi_0^2} \right) P[X, \phi_0] \right\}. \quad (16)$$

By demanding that the equilibrium Boltzmann distribution function that follows from Eq. (8), given by

$$P_{\text{eq}} \propto e^{-V_{\text{eff}}/k_B T}, \quad (17)$$

is a time-independent solution of the above Fokker-Planck equation, we find the strength of the thermal fluctuations as

$$\sigma = 2\alpha k_B T L_z / \hbar N. \quad (18)$$

We see that the noise obeys the fluctuation-dissipation theorem with an effective temperature $T L_z / N$. The temperature is therefore effectively reduced by the magnetic moment density in the domain wall line.

B. Results

Two of us analyzed the model in Eqs. (13) and (14) in the presence of extrinsic pinning.²¹ In this section, we focus instead on the clean situation, in which $V_{\text{dis}} = 0$ everywhere. In the $T = 0$ case, the domain wall line will stay straight because the force on each point is exactly the same. Specializing to $\beta = 0$, we find that there is a critical current $v_{s, \text{crit}} = \lambda K_{\perp} / \hbar$. Below this critical current, the domain wall will not be able to acquire a finite drift velocity. This phenomenon is usually called intrinsic pinning,²⁶ and it does not occur for $\beta \neq 0$. Above the critical current, the domain wall will acquire an average drift velocity, given by

$$\langle \dot{X} \rangle = -\frac{1}{(1 + \alpha^2)} \sqrt{v_s^2 - v_{s, \text{crit}}^2}. \quad (19)$$

In the presence of thermal fluctuations we can no longer assume that the domain wall remains straight, and we need to go through a rather more elaborate procedure to find the average drift velocity. More specifically, if there

are thermal fluctuations, we can differentiate between the *flow* regime above $v_{s,\text{crit}}$, for which Eq. (19) still approximately applies, and the *thermal* regime below $v_{s,\text{crit}}$, in which the speed is finite, but goes with a different power law.

To find the behavior in the thermally assisted regime, we start by rewriting the Langevin equations to find just one equation for $\phi_0(z, t)$. We then specialize to the case without an external magnetic field, with $\beta = 0$, and take $1 + \alpha^2 \simeq 1$. We assume that $X'' \simeq 0$ because there is no potential that couples to X and find

$$\dot{\phi}_0 = 2\alpha \frac{J}{\hbar} \phi_0'' - \frac{\alpha K_{\perp}}{\hbar} \sin(2\phi_0) - \frac{\alpha v_s}{\lambda} + \eta_X - \alpha \eta_{\phi_0}, \quad (20)$$

which describes the motion of a string in a tilted washboard potential, a problem that was investigated before in a different context by Büttiker and Landauer.²⁸ For $v_s < v_{s,\text{crit}}$, the string propagates by thermal activation. This occurs due to the formation of a nucleus, or of a kink-antikink pair in the string. That is, part of the string is moved over the potential barrier due to thermal activation. If this nucleus is large enough, the kink and antikink will proceed to move apart from one another, and the string propagates to the next potential valley. Two factors are important: the energy barrier ΔE that needs to be overcome to generate a sufficiently large nucleus, and the propagation velocity of the kinks (and antikinks).

Let us start with the former. It is given by $\Delta E/E_0 = \sqrt{J/K_{\perp}} \int (d\phi_{0,N}/dz)^2 dz$, where $\phi_{0,N}$ is a time-independent solution of the differential equation $(J/K_{\perp})(d^2\phi_{0,N}/dz^2) = \sin(\phi_{0,N}) - v_s/v_{s,\text{crit}}$, and represents a stationary configuration, corresponding to the motion from a local maximum and back. In the above, ΔE is given in units of $E_0 = \alpha\sqrt{JK_{\perp}}/(2\lambda)$. The result is shown in Fig. 1. In the limit that we are close to the

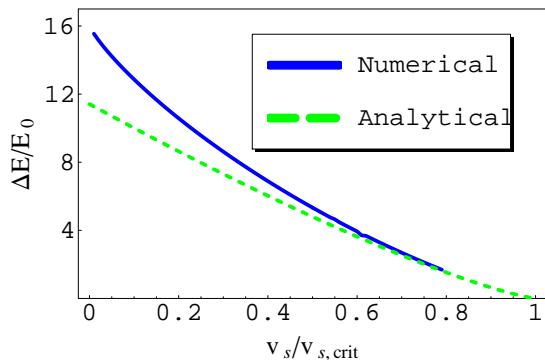


FIG. 1: (Color online) The energy barrier $\Delta E/E_0$ necessary to generate a nucleus large enough for the kink and antikink to propagate as a function of $v_s/v_{s,\text{crit}}$. The solid line was found by numerical calculation. The dashed line corresponds to Eq. (21).

critical current, i.e. that $(v_{s,\text{crit}} - v_s)/v_{s,\text{crit}} \ll 1$, we can solve for ΔE exactly and find²⁸

$$\Delta E = \frac{24}{5} \alpha \frac{\sqrt{JK_{\perp}}}{\lambda} \left(1 - \frac{v_s}{v_{s,\text{crit}}}\right)^{5/4}. \quad (21)$$

This formula indeed fits very well to the tail of our numerical curve. Note that the energy barrier remains finite as $v_s \rightarrow 0$. The difference between the above formula and the numerical solution is at most 25%, suggesting we may use Eq. (21) to estimate the qualitative behavior of domain wall motion even at lower values of $v_s/v_{s,\text{crit}}$. In the limit that $v_s \rightarrow 0$ we have that $\Delta E \propto v_s \log v_s$. This limit is not shown in Fig. 1 as it applies only for v_s very close to zero.

The other important quantity is the velocity at which the kink and antikink move away from one another. This velocity is found numerically by solving the equation

$$\phi_0'' + \frac{u}{u_0} \phi_0' - \sin \phi_0 + \frac{v_s}{v_{s,\text{crit}}} = 0, \quad (22)$$

with $u_0 = 2\lambda E_0/\hbar$, and finding the u for which the solution $\phi_0(z)$ which starts out at $\phi(0) = \arcsin(v_s/v_{s,\text{crit}})$ will go away from that point, and return to $\arcsin(v_s/v_{s,\text{crit}})$ at $z \rightarrow \infty$. The universal curve for this velocity is shown in Fig 2.

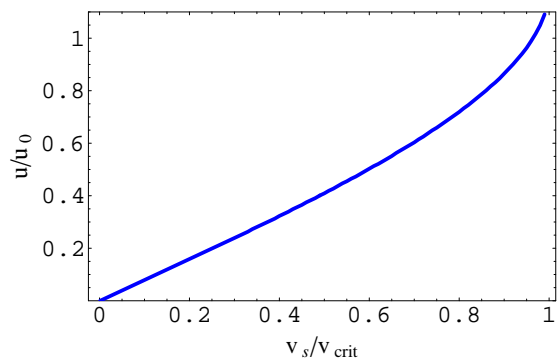


FIG. 2: Velocity of the kink (equal to minus the velocity of the antikink), as a function of current.

The probability of creating sufficiently large nuclei follows an Arrhenius law $j \propto \exp[-\Delta E/k_B T]$. We now have all the necessary ingredients to find the average velocity of the string, which is proportional to \sqrt{uj} . In the limiting case where the current is close to the critical one, we have that²⁸

$$\langle \dot{X} \rangle = 5^{3/4} (6\pi)^{1/4} \frac{2\lambda K_{\perp}}{\hbar} \sqrt{u} e^{-\frac{\Delta E}{2k_B T}} \left(\frac{\Delta E}{k_B T} \right)^{1/4} \left[1 - \left(\frac{v_s}{v_{s,\text{crit}}} \right)^2 \right]^{3/8}, \quad (23)$$

where u is a function of $v_s/v_{s,\text{crit}}$ as in Fig. 2. In Fig. 3, we have plotted this velocity for different temperatures.

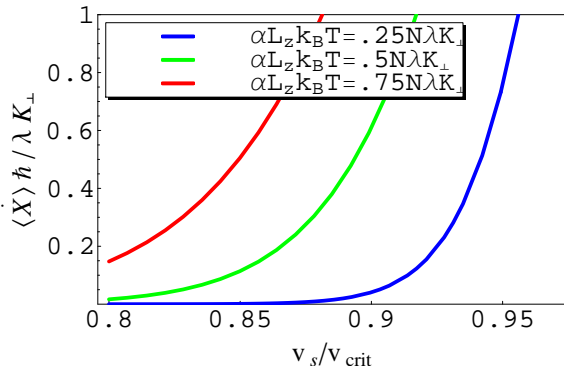


FIG. 3: (Color online) Velocity of the domain wall line as a function of current, for different values of T .

C. Experimental Status

In many experiments, the nanostrip is sufficiently narrow that we can neglect deformations of the domain wall line and approximate it as being rigid, an approximation we treat in the next section. However, Yamanouchi *et al.*²⁹ have observed in their experiments with magnetic semiconductors that the domain wall looks wedge-shaped in the current-induced case, suggesting that deformations play a role in wide enough nanostrips.

Yamanouchi *et al.* also found that the velocity of the domain wall obeys a scaling law. More specifically, they fitted their data with a creep-like scaling law $\log \dot{X} \propto v_s^{-\mu}$ with an exponent $\mu \simeq 0.33$. Recent experiments with ferromagnetic metals³⁰ have found the exponent $\mu \simeq 1/4$ which would imply²¹ that the dissipative spin-transfer torque dominates in the creep regime in this case.

III. RIGID DOMAIN WALLS

In this section, we simplify the model of domain-wall lines by assuming that the domain-wall coordinates are constant along the z direction, the domain wall is then rigid. This simplification allows us to obtain various results analytically.

A. Model

As mentioned before, rigid domain walls obey $X' = \phi'_0 = 0$, i.e., they are rigid in the z direction. We expect this approximation to hold in the limit when L_z is comparable to λ . We integrate Eqs. (13) and (14) over z (which is quite trivial since there are no z dependences anymore) to obtain the Langevin equations for a rigid domain wall (We use $\int dz \delta V[X(z)]/\delta X(z) \rightarrow \partial V(X)/\partial X$ and equivalently for ϕ_0)

$$\dot{\phi}_0 + \alpha \frac{\dot{X}}{\lambda} = \frac{-\lambda}{\hbar N} \frac{\partial V_{\text{rigid}}}{\partial X} + \tilde{\eta}_X, \quad (24)$$

$$\frac{\dot{X}}{\lambda} - \alpha \dot{\phi}_0 = \frac{1}{\hbar N} \frac{\partial V_{\text{rigid}}}{\partial \phi_0} + \tilde{\eta}_{\phi_0}. \quad (25)$$

We integrate the total potential in Eq. (15) to find (note that $X' = \phi'_0 = 0$)

$$V_{\text{rigid}} = -\hbar N \left[\frac{K_{\perp}}{2\hbar} \cos(2\phi_0) + \frac{gB_z X}{\hbar} \lambda + \frac{v_s}{\lambda} \left(\beta \frac{X}{\lambda} - \phi_0 \right) \right] + V_{\text{dis}}(X, \phi_0). \quad (26)$$

The stochastic correlations are found from

$$\begin{aligned} \langle \tilde{\eta}_i(t) \tilde{\eta}_j(t') \rangle &= \frac{1}{L_z^2} \langle \int_0^{L_z} dz \int_0^{L_z} dz' \eta_i(z, t) \eta_j(z', t') \rangle \\ &= \frac{2\alpha k_B T}{\hbar N} \delta_{ij} \delta(t - t'). \end{aligned} \quad (27)$$

In our model, rigid domain-walls obey the fluctuation-dissipation theorem with effective temperature T/N , i.e., the temperature is effectively reduced by the number of magnetic moments in the domain wall.

B. Results

1. Clean system, intrinsic pinning

We first focus on the case that the extrinsic pinning is zero. Substitution of \dot{X} from Eq. (24) into Eq. (25) then provides us with an equation that is independent of X . Using the equilibrium solution of Eq. (16), we find the average velocity of the chirality $\langle \dot{\phi}_0 \rangle$. With this result and Eq. (24), we compute average drift velocities

$$\alpha \frac{\langle \dot{X} \rangle}{\lambda} = -\langle \dot{\phi}_0 \rangle + \beta \frac{v_s}{\lambda} + \frac{gB_z}{\hbar}, \quad (28)$$

where the average chirality velocity is given by²⁷ (we omit a factor $1 + \alpha^2 \simeq 1$)

$$\langle \dot{\phi}_0 \rangle = \frac{-2\pi(e^{H_{\text{eff}}} - 1)\alpha k_B T / \hbar N}{\int_0^{2\pi} d\phi e^{-\Phi(\phi)} \left[\int_0^{2\pi} d\phi' e^{\Phi(\phi')} + (e^{H_{\text{eff}}} - 1) \int_0^\phi d\phi' e^{\Phi(\phi')} \right]}. \quad (29)$$

In this expression, the dimensionless effective potential is given by

$$\Phi(\phi_0) = \frac{N\hbar}{k_B T} \left[\frac{\sigma H_{\text{eff}} \phi_0}{4\pi L_z \alpha} - \frac{K_\perp}{2\hbar} \cos(2\phi_0) \right], \quad (30)$$

and the dimensionless effective field is defined as $H_{\text{eff}} = 4\pi L_z [(\alpha - \beta)v_s/\lambda - gB_z/\hbar]/\sigma$. The expressions in Eqs. (28) and (29) generalize the results by Duine *et al.*,²² to include external magnetic fields and $\beta \neq 0$.

In the field-driven case, we set $v_s = 0$ to find the behavior in Fig. 4. In the calculations, we use a fixed value for the damping parameter $\alpha = 0.02$ and several values for the temperature. At zero temperature, the drift ve-

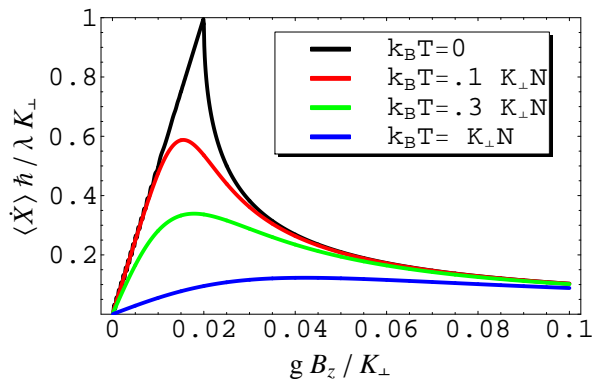


FIG. 4: (Color online) Field-driven domain-wall motion for several temperatures. We set $v_s = 0$ and take $\alpha = 0.02$.

locity depends on the external magnetic field linearly as $\langle \dot{X} \rangle = \lambda(gB_z/\hbar)/\alpha$ up to a critical value $H_{\text{cr}} = \alpha K_\perp/\hbar$. At this point, the domain wall starts precessing, causing the Walker-breakdown. This behavior was originally predicted by Schryer and Walker,³¹ and was subsequently observed, e.g. by Beach *et al.*³² From Fig. 4 we see that for nonzero temperatures, the Walker breakdown smoothens out. For $T \rightarrow \infty$, it fully disappears, and we find that the domain-wall velocity is linear with the field for all fields. We note that temperature only has an effect on the drift velocity for small fields. For very large external fields, the drift velocity is for all temperatures linear with the field and obeys $\langle \dot{X} \rangle = \alpha\lambda(gB_z/\hbar)$.

For the purely current-driven case, where we set $B_z = 0$, the relative values of α and β determine the sign of the contribution due to the current to the effective force. Again, we set $\alpha = 0.02$ and choose several values for β

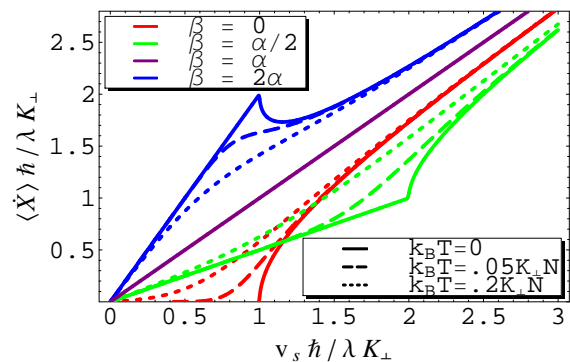


FIG. 5: (Color online) Current-driven domain-wall motion for several temperatures and several values of β . We set $B_z = 0$ and take $\alpha = 0.02$.

and for the temperature. It is indeed seen in Fig. 5 that the behavior of the average drift velocity for $\beta < \alpha$ is very different from $\beta > \alpha$. In the limiting case $\beta = 0$, we see that there is a critical current $v_{s,\text{crit}} = K_\perp \lambda/\hbar$, in agreement with Eq. (19). In the large β limit, we recognize a Walker-breakdown-like behavior, just like the behavior found in purely field-driven domain-wall motion. For very large currents, the drift velocity acquires a linear dependence on the spin current $\langle \dot{X} \rangle = v_s$ for all values of β and for all temperatures.

2. Extrinsic pinning

Domain-wall pinning is of practical interest. Control of domain walls is achieved by pinning the domain wall in a position by means of, for example, a deformation in the material. In nanowires or thin metal strips, dents in the sample act as an intended pinning potential. A thorough understanding of depinning times is especially important in systems that are relevant for technological applications, such as data-storage devices.

To incorporate pinning in our theory, we add a pinning potential V_{pin} to the potential V_{rigid} in Eqs. (24) and (25). A pinning potential that is due to a deformation in the material can be obtained through energy analysis. We discern between two types of deformations: symmetric and asymmetric notches. The sample we have in mind is a thin strip of ferromagnetic or semiconductor material, where the notches are little dents on the sides of the strip. In the case of symmetric notches, there is a dent on both sides of the sample. If there is only a dent on one side, we have an asymmetric notch. It turns out that symmetric pinning sites can effectively be described by a quadratic-well potential in the X direction,¹⁸ that is independent of the chirality. For asymmetric notches, the pinning potential also has a chirality dependence.¹²

As an example, we consider the symmetric notch. If we add a X dependent symmetric-notch contribution to Eqs. (24) and (25), we see that the pinning contribution

in Eq. (25) vanishes. Because of the explicit X dependence in Eq. (24), the system can no longer be described by a probability distribution that depends on the variable ϕ_0 only. Therefore, all terms in the Fokker-Planck equation (16) need to be taken into account, and we are not able to find an analytic solution to the full problem. We can, however, compute depinning times using Kramer's escape-rate theory.

The potential that Tataro *et al.*²⁶ proposed for a symmetric notch has a kink at the sides, which makes it less suitable for escape-rate computations. We therefore use a very similar, but smooth potential

$$V_{\text{pin}}^{\text{S}} = \frac{NV_0}{2} \left[2 \left(\frac{X}{\xi} \right)^2 - \left(\frac{X}{\xi} \right)^4 \right], \quad (31)$$

where $V_0/2$ is the depth and 2ξ is the width of the potential well.

We compute depinning times for the pinning potential in Eq. (31) using Kramer's escape-rate theory which states that the depinning time is proportional to $\log(\tau\omega_0) = \Delta V/\hbar k_{\text{B}}T$, where $\omega_0 \propto V_0/\hbar$ is an attempt frequency and ΔV is the height of the potential barrier that has to be overcome. We determine the positions of the potential minimum and the saddle through variation of the potential $V_{\text{rigid}} + V_{\text{pin}}$. Substitution of these coordinates provides us with the potential difference ΔV . The depinning time for driving current and field is found as $\log \tau \propto \Delta V \propto -(gB_z/\hbar + \beta v_s/\lambda)$. Note that if $\beta = 0$, the depinning time is independent of the applied current within this approximation.

3. Disorder potential

The final potential that we consider is a disorder potential. Due to, for example, roughness on the edges of a sample, there is a random pinning potential $V_{\text{dis}}(X)$ that is felt by the domain wall. We consider a situation of strong pinning of the angle ϕ_0 such that $\langle \dot{\phi}_0 \rangle = 0$ (See Ref. [23] for an extensive analysis including the dynamics of this angle). This would be the case for fields below Walker breakdown and currents below $v_{\text{s,crit}}$. The equation of motion for the coordinate X is then found from Eq. (24) to be

$$\alpha \frac{\dot{X}}{\lambda} = \beta \frac{v_s}{\lambda} + \frac{gB_z}{\hbar} - \frac{\lambda}{\hbar N} \frac{\partial V_{\text{dis}}(X)}{\partial X} + \tilde{\eta}_X. \quad (32)$$

The disorder potential $V_{\text{dis}}(X)$ that enters the equations of motion is characterized by certain spatial correlations $\overline{[V_{\text{dis}}(X) - V_{\text{dis}}(X')]^2} = \Delta |(X - X')/\lambda|^\gamma$. In this expression, the line denotes an average over the disorder, and $\Delta > 0$ is a measure for the strength of the disorder potential. The exponent γ characterizes the nature of the correlations. In general, there are two ways of obtaining a disorder potential: by applying a random field, or by randomizing locally the strength of certain coupling constants in the system, for example the anisotropy or the

spin stiffness. The former is called random field disorder and gives rise to correlations with $\gamma = 1$, whereas the latter is called random bond disorder with exponent $\gamma = 0$. For both limits, Le Doussal and Vinokur³³ have obtained expressions for depinning times for a zero-dimensional object (in our one-dimensional model, the domain wall itself is described as a point at position $\{X, \phi_0\}$ with dimension zero).

For random field disorder ($\gamma = 1$), Le Doussal and Vinokur find that the drift velocity is zero up to some critical driving current and/or field $F_c \propto \Delta/T$, and is then linear with the driving force

$$\frac{\langle \dot{X} \rangle}{\lambda} = \frac{\beta v_s}{\lambda} + \frac{gB_z}{\hbar} - F_c. \quad (33)$$

For random bond disorder ($\gamma = 0$) they find that the drift velocity obeys

$$\langle \dot{X} \rangle \propto \frac{(\beta v_s/\lambda + gB_z/\hbar)^{z-1}}{\Gamma(z-1)T^{z+2}}, \quad (34)$$

where $z = 2 + \Delta/2(k_{\text{B}}T)^2$ is the so-called dynamical exponent and $\Gamma(z)$ is the gamma function. Surprisingly, they find that for $0 < \gamma < 1$ the results turn out to resemble the results obtained for higher-dimensional objects, i.e. Le Doussal and Vinokur find a creep scaling law with a certain creep exponent

$$\langle \dot{X} \rangle \propto \left(\frac{\beta v_s/\lambda + gB_z/\hbar}{F_c} \right)^{\frac{z-1-\gamma/2}{1-\gamma}} \times \exp \left[-(1-\gamma) \left(\frac{\beta v_s/\lambda + gB_z/\hbar}{\gamma F_c} \right)^{\frac{-\gamma}{1-\gamma}} \right], \quad (35)$$

where $F_c \propto T[\Delta/2(k_{\text{B}}T)^2]^{1/\gamma}$ is a characteristic critical driving force. Note that the creep exponent $(z-1-\gamma/2)/(1-\gamma)$ is always larger than 1 for $0 < \gamma < 1$.

C. Comparison with other work

To compute drift velocities at finite temperature, we have expanded the theory proposed by Duine *et al.*⁸ to include external magnetic fields in addition to driving currents. Other theoretical work is done by Tataro *et al.*²⁴ and by Martinez *et al.*²⁵ Here, we compare our results with the results by Martinez *et al.*

In order to write Eqs. (24) and (25) in terms of the coordinate X only, Martinez *et al.* assume ϕ_0 to be small such that $\sin 2\phi_0 \simeq 2\phi_0$. Note that this assumption only holds when $B_z \ll gK_{\perp}$ and/or $v_s \ll v_{\text{s,crit}}$ for $\beta \neq 0$. If, however, we do make this assumption, and differentiate Eqs. (24) and (25) with respect to time, we find

$$\frac{\ddot{X}}{\lambda} = \alpha \ddot{\phi}_0 + 2\dot{\phi}_0 \frac{K_{\perp}}{\hbar}, \quad (36)$$

$$\ddot{\phi}_0 = -\alpha \frac{\ddot{X}}{\lambda}, \quad (37)$$

where we omitted the stochastic terms. We now substitute Eqs. (24) and (37) in Eq. (36) and like Martinez *et al.* add a stochastic term to find

$$(1 + \alpha^2) \frac{\hbar}{2K_{\perp}} \frac{\ddot{X}}{\lambda} = -\alpha \frac{\dot{X}}{\lambda} + \beta \frac{v_s}{\lambda} + \frac{gB_z}{\hbar} + \zeta_{\text{th}}. \quad (38)$$

The correlations of the stochastic force are, according to Martinez *et al.*, given by

$$\langle \zeta_{\text{th}}(t) \zeta_{\text{th}}(t') \rangle = \sigma \delta(t - t'), \quad \langle \zeta_{\text{th}}(t) \rangle = 0. \quad (39)$$

From the fluctuation-dissipation theorem, they infer that $\sigma \propto N\alpha k_B T$. An easy way to obtain the Fokker-Planck equation is to introduce a new variable $v = \dot{X}$,²⁷ such that we have two Langevin equations

$$\dot{X} = v, \quad (40)$$

$$(1 + \alpha^2) \frac{\hbar}{2K_{\perp}} \frac{\dot{v}}{\lambda} = -\alpha \frac{v}{\lambda} + \beta \frac{v_s}{\lambda} + \frac{gB_z}{\hbar} + \zeta_{\text{th}}. \quad (41)$$

Note that the above equations have to be solved with the initial conditions $\dot{X}(t=0) = v(t=0) = v_s$ to include the reactive spin-transfer torque. The Fokker-Planck equation generated by these Langevin equations is given by (we omit a factor $1 + \alpha^2 \simeq 1$)

$$\begin{aligned} \frac{\partial P[X, v]}{\partial t} &= -\frac{\partial}{\partial X} (vP[X, v]) \\ &- \frac{2K_{\perp}}{\hbar} \frac{\partial}{\partial v} \left[-\alpha \frac{v}{\lambda} + \beta \frac{v_s}{\lambda} + \frac{gB_z}{\hbar} + \frac{\sigma K_{\perp}}{\hbar} \frac{\partial}{\partial v} \right] P[X, v]. \end{aligned} \quad (42)$$

This Fokker-Planck equation is satisfied by a Boltzmann equilibrium distribution that has the same potential energy as Eq. (26) for $\phi_0 = 0$, but with an additional kinetic energy $\hbar v^2 / K_{\perp}$. The exact form of the stochastic strength is $\sigma = \alpha k_B T / NK_{\perp}$. We conclude that this procedure complies with our model for a small range of applicability.

Several field-driven domain-wall motion experiments have been performed in ferromagnetic metallic materials.^{18,32} Clear Walker-breakdown behavior is observed, but the peak is not smoothed like our theory predictions. Estimates by Duine *et al.*²² show that room temperature, at which these experiments were performed, leads to an effective temperature $k_B T / NK_{\perp} \simeq 10^{-3}$ for ferromagnetic metals. Our prediction is therefore indistinguishable from the zero-temperature curve in Fig. 4. The reason for this low effective temperature is the fact that the number of particles in the domain wall is relatively high in a ferromagnetic metal. In magnetic semiconductors, however, not all magnetic moments participate in the magnetization, reducing the number of magnetic moments in a domain wall by up to a factor ~ 100 , thereby greatly increasing the effective temperature. From Fig. 4 we see that an effective temperature $k_B T / NK_{\perp} \simeq 10^{-1}$ should be distinguishable from the

zero-temperature curve. We predict therefore that the influence of thermal effects on Walker breakdown should be observable with field-driven domain walls in clean magnetic semiconductors.

Escape time studies have been performed on narrow domain walls by Ravelosana *et al.*¹³ They indeed find that the logarithm of the (average) escape time decreases linearly with the applied current. Since the current dependence of the logarithm of the escape time is determined by β , we can estimate the value of β from their curve, and we find that it is of the order $\beta \sim 10^{-2}$, i.e. of the order of the damping parameter α , in agreement with theoretical expectations.

IV. VORTEX DOMAIN WALLS

In this section we consider the limit of the domain-wall line that corresponds to vortex domain walls and derive several analytical and numerical results.

A. Model

Vortex domain walls are described by making the *ansatz* for the z dependence of the chirality

$$\phi_0 = 2 \arctan e^{\pm[z - Z(t)]/\kappa}. \quad (43)$$

The coordinate $Z(t)$ plays a similar role as $X(t)$, and the width of the vortex domain wall $\kappa = \sqrt{J/K_{\perp}}$ in the z direction is the equivalent of the width λ in the x direction. The coordinates $\{X(t), Z(t)\}$ now determine the position of the vortex at time t .

In principle, we should consider boundary conditions in the z direction. We deal with this problem by assuming $\kappa/L_z \rightarrow 0$, in which limit the *ansatz* reduces to $\phi_0 \simeq \pi/2 \pm \{\theta[z - Z(t)] - 1/2\}\pi$, with $\theta(x)$ the Heaviside step function. The drawback is that we are now neglecting all boundary effects. The \pm sign is the product of the chirality and charge in the *ansatz* and determines whether we have a clockwise or counterclockwise rotation in the vortex domain wall, and is usually denoted as the Skyrmion number $s \in \{-1, 1\}$. We note that the vortex domain wall is now fully characterized by its position $\{X(t), Z(t)\}$, its dimensions ($\kappa \times \lambda$), this Skyrmion number s and the number of magnetic moments in the vortex $4\kappa\lambda L_y/a^3 = 2\kappa N/L_z$.

We apply the simplified *ansatz* to the action in Eq. (9) to find an action for a vortex domain wall in terms of the collective coordinates $X(t)$ and $Z(t)$

$$\begin{aligned} S_{\text{vor}}[X, Z] &= \\ &- \hbar N \int dt \left(s\pi \frac{Z}{L_z} \frac{\dot{X}}{\lambda} - \frac{gB_z}{\hbar} \frac{X}{\lambda} - s\pi \frac{v_s}{\lambda} \frac{Z}{L_z} \right). \end{aligned} \quad (44)$$

The dissipation function in Eq. (10) is also written in terms of the new coordinates, however, we need to take

into account the full ansatz in Eq. (43) in order to find the κ dependence in the last term

$$R_{\text{vor}}[X, Z] = \frac{\alpha \hbar N}{2} \int dt \left[\left(\frac{\dot{X}}{\lambda} - \frac{\beta v_s}{\alpha \lambda} \right)^2 + \frac{2\dot{Z}^2}{\kappa L_z} \right]. \quad (45)$$

Variation of the functionals in Eqs. (44) and (45) provides us with the Langevin equations for a vortex domain wall

$$-s\pi \frac{\dot{Z}}{\kappa} + \frac{\alpha L_z}{\kappa} \frac{\dot{X}}{\lambda} = \frac{\beta L_z}{\kappa} \frac{v_s}{\lambda} + \frac{L_z}{\kappa} \frac{gB_z}{\hbar} + \eta_X^V, \quad (46)$$

$$s\pi \frac{\dot{X}}{\lambda} + 2\alpha \frac{\dot{Z}}{\kappa} = s\pi \frac{v_s}{\lambda} + \eta_Z^V, \quad (47)$$

where we have again added stochastic forces to model thermal effects. We see that the effective dampings are given by $\alpha_X = \alpha L_z / \kappa$ and $\alpha_Z = 2\alpha$. We write the right-hand side of Eqs. (46) and (47) in terms of a total potential

$$V_{\text{vortex}} = -\hbar N \left[\frac{v_s}{\lambda} \left(\beta \frac{X}{\lambda} + s\pi \frac{Z}{L_z} \right) + \frac{gB_z}{\hbar} \frac{X}{\lambda} \right], \quad (48)$$

Note that this potential is also obtained by inserting the *ansatz* in Eq. (15). With these identifications, we can again write the Langevin equations (46) and (47) in the more suggestive form

$$s\pi \frac{\dot{Z}}{\kappa} - \alpha_X \frac{\dot{X}}{\lambda} = \frac{L_z}{\kappa N} \frac{\lambda}{\hbar} \frac{\partial V_{\text{vortex}}}{\partial X} + \eta_X^V, \quad (49)$$

$$s\pi \frac{\dot{X}}{\lambda} + \alpha_Z \frac{\dot{Z}}{\kappa} = -\frac{L_z}{\kappa N} \frac{\kappa}{\hbar} \frac{\partial V_{\text{vortex}}}{\partial Z} + \eta_Z^V. \quad (50)$$

Note that the prefactor $L_z / N\kappa$ is proportional to the inverse of the number of magnetic moments in the vortex domain wall. Using the Fokker-Planck method outlined in section II, we find that the probability distribution function P does not satisfy Boltzmann equilibrium $P \propto \exp[-V_{\text{vortex}} / \hbar k_B T]$ if we assume that the fluctuations in the X and Z direction have the same strength. However, we write down a more general Fokker-Planck equation than the one in Eq. (16), in terms of stochastic correlations $\langle \eta_i^V(t) \eta_j^V(t') \rangle = \sigma_{ij} \delta(t - t')$. Again, we demand the Boltzmann equilibrium in Eq (17) to be a solution to the modified Fokker-Planck equation, which yields complicated equations that can be solved. Up to second order in the small parameter α , we find that the stochastic correlations must obey

$$\langle \eta_i^V(t) \eta_j^V(t') \rangle = \sigma_i \delta_{ij} \delta(t - t'), \quad (51)$$

where the indices denote $i \in \{X, Z\}$ and

$$\sigma_X = 2\alpha_X \frac{k_B T L_z}{\hbar N \kappa}; \quad \sigma_Z = 2\alpha_Z \frac{k_B T L_z}{\hbar N \kappa}. \quad (52)$$

In these relations, we recognize the fluctuation-dissipation theorem with effective temperature $T_{\text{eff}} =$

$TL_z / N\kappa$. The reduction by the factor $\kappa N / L_z$ is caused by the fact that the number of microscopic degrees of freedom is proportional to this factor. Note that, because the damping is anisotropic, it is also necessary to introduce anisotropy in the fluctuations.

From the form of Eqs. (49) and (50), it is clear that we reach the isotropic case for $\alpha_X = \alpha_Z$, i.e. when we demand that $L_z = 2\kappa$. Note that then also $\sigma_X = \sigma_Z$ and that the reduction of the effective temperature is now proportional to N . That this is indeed the isotropic case is also seen from the fact that now the coordinates X/λ and Z/κ are treated on equal footing in the dissipation functional in Eq. (45).

If we also demand that $\lambda = \kappa$, our model describes circular vortices, that furthermore occupy the entire width of the strip. This case is similar to the zero-temperature results of Shibata *et al.*¹⁵ on the current-induced vortex displacement in a magnetic nanodisk, and their equations of motion correspond to ours in the case that $\beta = 0$ and $B_z = 0$.

To include extrinsic pinning in our model, we again add a pinning potential to the potential V_{vortex} . As an example, we will consider a circularly symmetric pinning potential, quadratic in both X and Z , and bounded at a certain radius ξ

$$V_{\text{pin}}^V = N \frac{V_0}{2} \left[\left(\frac{X}{\xi} \right)^2 + \left(\frac{Z}{\xi} \right)^2 \right] \theta(X^2 + Z^2 - \xi^2). \quad (53)$$

B. Results

1. Zero temperature without extrinsic pinning

When there are no external fields or pinning potentials, we can read off the $T = 0$ behavior directly from Eqs. (46) and (47). For instance, it is clear that under the influence of a current to the right, the domain wall will move to the right also, and its speed in the x -direction will be directly proportional to the current, as can be seen in

$$\dot{X} = \frac{1 + \frac{2L_z}{\pi^2 \kappa} \alpha \beta}{1 + \frac{2L_z}{\pi^2 \kappa} \alpha^2} v_s. \quad (54)$$

Note that if $\beta = \alpha$, the velocity of the domain wall will be exactly equal to the velocity of the current. For the transverse velocity \dot{Z} , we get

$$\dot{Z} = \frac{-sL_z(\beta - \alpha)v_s}{\lambda(\pi + \frac{2L_z}{\pi\kappa}\alpha^2)}. \quad (55)$$

The direction of motion in the z -direction depends on the skyrmion number s , and also on the sign of $\beta - \alpha$, and the magnitude is proportional to v_s . Theoretically, if $\beta = \alpha$, the vortex core would move in a straight line, i.e. the center of the vortex would not get a transverse displacement. Note that there is no intrinsic pinning in

the case of a vortex domain wall, not even if $\beta = 0$. For $\beta = \alpha = 0$, $\langle \dot{X} \rangle = \frac{\lambda}{\kappa} v_s$, showing that the shape of the vortex domain wall has an influence on the motion as well.

2. Zero temperature with extrinsic pinning

We will now investigate what happens if there is a pinning potential of the form in Eq. (53). If the potential is not bounded (i.e. if the step function is absent), $T = 0$ and $H_{\text{ext}} = 0$, the solutions can be found analytically, and they describe a circular motion ending at a fixed point. As we can read from the formulas, these fixed points will be at $X = \beta v_s \hbar \xi^2 / (\lambda^2 V_0)$ and $Z = s \pi v_s \hbar \xi^2 / (\lambda L_z V_0)$. Note that only the former depends on β . This agrees with our physical intuition that β tilts the potential landscape in the X -direction, but that it has no effect in the Z -direction.

When the potential is bounded there is a critical current for depinning the domain wall. We cannot find this current precisely using analytic calculations, but we can however make a rough estimation if we take the current for which the equilibrium position falls outside the boundary as an indication. This will naturally overestimate the critical current since the domain wall precesses after the current is switched on, but it is a good approximation for the upper boundary. We find

$$v_{s,\text{crit}} < \frac{\lambda^2 V_0 L_z}{\hbar \xi} \sqrt{\frac{1}{L_z^2 \beta^2 + \lambda^2 \pi^2}}. \quad (56)$$

Numerical calculations can give us more precise results. For instance, for a symmetric domain wall (i.e. $\kappa = \lambda$) with $L_z = 100\lambda$, $\xi = \lambda$, and $\beta = 0$, we find $v_{s,\text{crit}} \simeq 21.78\lambda V_0/\hbar$, while the analytical upper bound found with the formula above is $v_{s,\text{crit}} < 31.831\lambda V_0/\hbar$. Numerical calculations also give us the escape time at $v_{s,\text{crit}}$, which is approximately $0.074\hbar/V_0$ (for $\beta = 0$). Eq. (56) suggests that the critical current is proportional to $1/\beta$. Fig. 6 shows both Eq. (56) and the numerical results for the aforementioned values of κ , L_z and ξ .

3. Escape rate at finite temperature

We now include thermal fluctuations. To give some insight into the motion of the domain wall in this case, we have plotted a possible solution to the Langevin Eqs. (49) and (50) in Fig. 7. The current here is just under the critical one, $k_B T L_z = NV\kappa$, and we are looking at a symmetric vortex with $L_z = 100\lambda$.

We next determine the escape time (i.e. the time it takes for the domain wall to move outside the boundary of the pinning potential) as a function of the current, and its dependence on temperature. As the average escape time is rather hard to determine and as the escape times

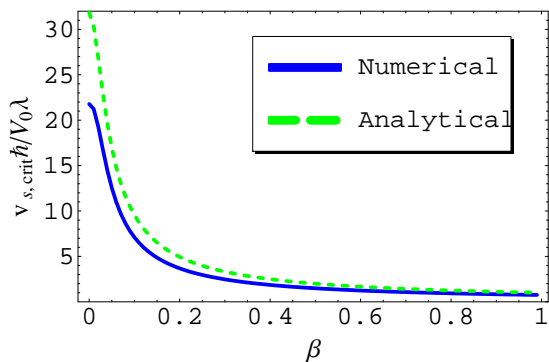


FIG. 6: (Color online) Critical current as a function of the dissipative spin-transfer torque parameter β .

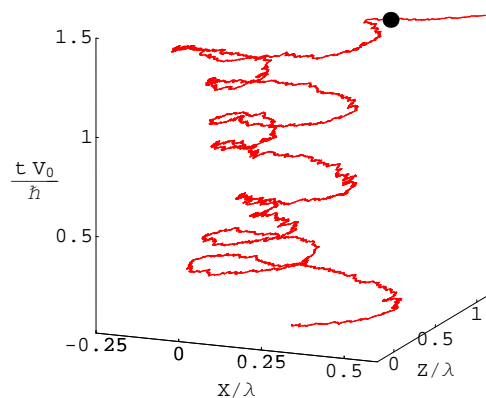


FIG. 7: A possible trajectory of a vortex domain wall in the presence of the pinning potential given by Eq. (53) with $k_B T L_z = NV\kappa$ and $\kappa = \lambda = L_z/100$. The black dot denotes the coordinates at which the vortex leaves the potential well, in this example at time $t \simeq 1.4\hbar/V_0$.

are distributed approximately exponentially, we have, for practical purposes, chosen the median escape time as an indicator. Median/ $\ln 2$ is then expected to be a good measure for the average escape time. The results, with the logarithm of the median escape time plotted against the current, are shown in Fig. 8.

Note that there is a clear distinction between the thermal regime and the slide regime. The behavior in the thermal regime can be fitted very well by an equation of the form $\exp[(a - bv_s/v_{s,\text{crit}})NV\kappa/k_B T L_z]$, with a and b two numerical factors. Fitting shows a to be of the order of 35, and b around 1.8. Hence we find that the logarithm of the escape time is proportional to current.

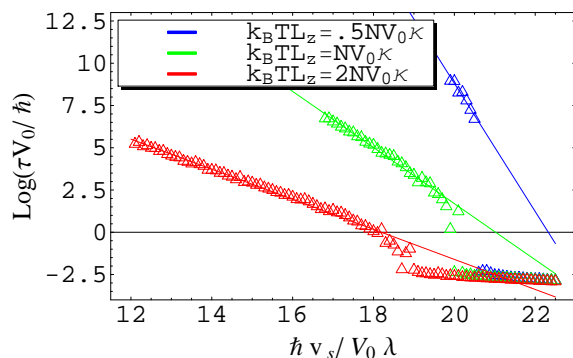


FIG. 8: Plot of the median escape time as a function of current, for three different values of the temperature.

C. Comparison with other work

Vortex domain walls are of great interest to experimentalists, because they are large enough to be visible with, for instance, scanning electron microscopy or magnetic force microscopy, and because their dynamics take place on observable time scales. Because many experiments are done with vortex domain walls, many theoretical models have been developed to describe them. He, Li and Zhang¹⁶ developed a 2D model for the vortex domain wall, while Shibata *et al.*¹⁵ described the current-induced motion of a circular magnetic vortex. The biggest difference between these two models and ours is that in their case, the vortex (domain wall) is not straight, but the equations of motion they find are remarkably similar to ours in the isotropic, symmetric case. The former group found the motion of the domain wall towards the edge of the nanostrip that our model also yields, and the latter paper predicted precession of the vortex domain wall in a potential. The model of Krüger *et al.*¹⁷ also predicts precession, of an elliptical shape, and our zero-temperature results are in agreement with theirs.

Current-driven vortex domain wall motion has indeed been observed by several experimental groups.^{20,34,35} Furthermore, Heyne *et al.*⁷ found, as expected, that the sign of the displacement in the Z -direction is determined by the skyrmion number and by the sign of $(\alpha - \beta)$. In the presence of pinning, precession of a magnetic vortex has indeed been found experimentally as well.¹⁹

No detailed experimental results on current-driven magnetic vortices at nonzero temperature have been reported.

V. CONCLUSIONS

We have presented a model for the driven motion of a domain-wall line at nonzero temperature, and analyzed

this model within several approximations.

First, we considered a general domain-wall line, which is described as a string in a tilted washboard potential. We computed the average drift velocity as a function of an applied current for currents lower than the critical current.

In the limit of rigid domain walls, we were able to find analytical expressions for drift velocities in the presence of thermal fluctuations. For the field-driven case, the well-known Walker-breakdown behavior smoothes for increasing temperature. In the current-driven case, the drift velocity depends heavily on the ratio of the dissipative spin-transfer torque parameter β and the Gilbert damping α . Here, the curves also smoothen with increasing temperature. As a result, we found no critical current for $\beta = 0$ at nonzero temperature. We also considered extrinsic pinning due to, for example, a notch in the sample. We found that the escape time is proportional to the exponent of the applied magnetic field and the dissipative spin-transfer torque. Comparison with experiment enabled us to estimate $\beta \sim 10^{-2}$ for that experiment¹³. Finally, we discussed the effect of a disorder potential on the dynamics of the rigid domain wall.

For vortex domain walls, we computed domain-wall velocities at zero temperature. In the presence of an extrinsic pinning potential, we found an analytic upper bound for the critical current. Numerical computation revealed critical currents just under this upper bound. At finite temperature, numerical simulations provided us with depinning times as a function of the applied current. We found two distinct regimes: one where thermal fluctuations dominate, and one where the current dominates. In the thermal regime, we found that the depinning time goes as $\log \tau \propto v_s/T$.

The models and results presented in this paper provide a simple framework for describing domain walls at nonzero temperature. Moreover, they are easily adapted to situations not discussed in this paper, such as different geometries. We hope that our results are confirmed with more experimental and numerical results in the near future.

Acknowledgments

This work was supported by the Netherlands Organization for Scientific Research (NWO), by the European Research Council (ERC) under the Seventh Framework Program (FP7), and by the National Science Foundation under Grant No. NSF PHY05-51164.

-
- * Electronic address: m.e.lucassen@uu.nl
- ¹ L. Berger, J. Appl. Phys. **55**, 1954 (1984).
 - ² P.P. Freitas and L. Berger, J. Appl. Phys. **57**, 1266 (1985).
 - ³ J.C. Slonczewski, J. Magn. Magn. Mater. **159**, L1 (1996).
 - ⁴ L. Berger, Phys. Rev. B. **54**, 9353 (1996).
 - ⁵ S. Zhang and Z. Li, Phys. Rev. Lett. **93**, 127204 (2004).
 - ⁶ S.E. Barnes and S. Maekawa, Phys. Rev. Lett. **95**, 107204 (2005).
 - ⁷ L. Heyne *et al.*, Phys. Rev. Lett. **100**, 066603 (2008).
 - ⁸ R.A. Duine, A.D. Núñez, J. Sinova and A. H. MacDonald, Phys. Rev. B **75**, 214420 (2007).
 - ⁹ T. Tserkovnyak, H.J. Skadsem, A. Brataas and G.E.W. Bauer, Phys. Rev. B **74**, 144405 (2006).
 - ¹⁰ H. Kohno, G. Tatara and J. Shibata, J. Phys. Soc. Jpn. **75**, 113706 (2006).
 - ¹¹ F. Piéchon and A. Thiaville, Phys. Rev. B **75**, 174414 (2007).
 - ¹² D. Petit, A.-V. Jausovec, D. Read, and R.P. Cowburn, J. Appl. Phys. **103**, 114307 (2008).
 - ¹³ D. Ravelosona, D. Lacour, J. A. Katine, B. D. Terris and C. Chappert, Phys. Rev. Lett. **95**, 117203 (2005).
 - ¹⁴ P. Bruno, Phys. Rev. Lett. **83**, 2425 (1999).
 - ¹⁵ J. Shibata, Y. Nakatani, G. Tatara, H. Kohno and Y. Otani, Phys. Rev. B **73**, 020403 (R) (2006).
 - ¹⁶ J.He, Z.Li and S. Zhang, Phys. Rev. B. **73**, 184408 (2006).
 - ¹⁷ B. Krüger, A. Drews, M. Bolte, U. Merkt, D. Pfannkuche and G. Meier, Phys. Rev. B **76**, 224426 (2007).
 - ¹⁸ M. Hayashi, L. Thomas, C. Rettner, R. Moriya, X. Jiang, and S.S.P. Parkin, Phys. Rev. Lett. **97**, 207205 (2006).
 - ¹⁹ M. Bolte *et al.*, Phys. Rev. Lett. **100**, 176601 (2008).
 - ²⁰ M. Kläui, P.-O. Jubert, R. Allenspach, A. Bischof, J. A. C. Bland, G. Faini, U. Rüdiger, C. A. F. Vaz, L. Vila and C. Vouille, Phys. Rev. Lett. **95**, 026601 (2005).
 - ²¹ R.A. Duine and C. Morais Smith, Phys. Rev. B **77**, 094434 (2008).
 - ²² R.A. Duine, A.S. Núñez and A.H. MacDonald, Phys. Rev. Lett. **98**, 056605 (2007).
 - ²³ V. Lecomte, S.E. Barnes, J.-P. Eckmann and T. Giamarchi, cond-mat.stat-mech/0903.0175 (2009).
 - ²⁴ G. Tatara, N. Vernier and J. Ferré, Appl. Phys. Lett. **86**, 252509 (2005).
 - ²⁵ E. Martinez, L. Lopez-Diaz, O. Alejos, L. Torres and C. Tristan, Phys. Rev. Lett. **98**, 267202 (2007).
 - ²⁶ G. Tatara and H. Kohno, Phys. Rev. Lett. **92**, 086601 (2004); **96**, 189702 (2006).
 - ²⁷ H. Risken, *The Fokker-Planck Equation* (Springer-Verlag, Berlin, 1984).
 - ²⁸ M. Büttiker and R. Landauer, Phys. Rev. A **23**, 1397 (1981).
 - ²⁹ M. Yamanouchi, J. Ieda, F. Matsukura, S. E. Barnes, S. Maekawa, H. Ohno, Science **317**, 1726 (2007).
 - ³⁰ T.A. Moore, I.M. Miron, G. Gaudin, G. Serret, S. Aufret, B. Rodmacq, A. Schuhl, S. Pizzini, J. Vogel and M. Bonfim, cond-mat.other/0812.1515 (2008).
 - ³¹ N.L. Schryer and L.R. Walker, J. Appl. Phys. **45**, 5406 (1974).
 - ³² G.S.D. Beach, C. Nistor, C. Knutson, M. Tsoi and J.L. Erskine, Nature Mat. **4**, 741 (2005).
 - ³³ P. Le Doussal and V.M. Vinokur, Physica C **254**, 63 (1995).
 - ³⁴ A. Yamaguchi, T. Ono, S. Nasu, K. Miyake, K. Mibu and T. Shinjo, Phys. Rev. Lett. **92**, 077205 (2004).
 - ³⁵ L. Thomas, M. Hayashi, X. Jiang, R. Moriya, C. Rettner and S.S.P. Parkin, Nature **443**, 197 (2006).